Carbohydrate Polymers 83 (2011) 1213–1217

Contents lists available at ScienceDirect

Carbohydrate Polymers

journal homepage: www.elsevier.com/locate/carbpol

Elastic modulus in the crystalline region and the thermal expansion coefficients of α-chitin determined using synchrotron radiated X-ray diffraction

Yu Ogawa [a], Ritsuko Hori [a], Ung-Jin Kim [b], Masahisa Wada [a,b,*]

[a] Department of Biomaterials Science, Graduate School of Agricultural and Life Sciences, The University of Tokyo, Yayoi 1-1-1, Bunkyo-ku, Tokyo 113-8657, Japan
[b] Department of Plant & Environmental New Resources, College of Life Sciences, Kyung Hee University, 1, Seocheon-dong, Giheung-ku, Yongin-si, Gyeonggi-do 446-701, Republic of Korea

ARTICLE INFO

Article history:
Received 3 August 2010
Received in revised form 1 September 2010
Accepted 14 September 2010
Available online 18 September 2010

Keywords:
α-Chitin
Crab tendon
Elastic modulus
Thermal expansion
Synchrotron X-ray diffraction

ABSTRACT

Crystalline, orientated fibers of α-chitin were obtained from the tendons of a snow crab (*Chionoecetes opilio*). The elastic modulus of the crystalline region along the fiber axis (E_l) and the thermal expansion coefficients (TECs) of α-chitin were measured using synchrotron X-ray diffraction. The E_l value of α-chitin was 59.3 ± 11.3 GPa, which was slightly larger than the value reported previously. This was because of the higher degree crystallinity of our sample and the use of synchrotron radiation as an X-ray source in this study. The linear TECs of the *a*-, *b*-, and *c*-axes were: $\alpha_a = 6.1 \times 10^{-5}\,^{\circ}C^{-1}$, $\alpha_b = 7.3 \times 10^{-5}\,^{\circ}C^{-1}$, and $\alpha_c = 2.1 \times 10^{-5}\,^{\circ}C^{-1}$, respectively. This anisotropic thermal expansion behavior, $\alpha_b > \alpha_a > \alpha_c$, was ascribed to the crystal structure and hydrogen bonding system of α-chitin. In addition, the volume TEC of α-chitin is reported for the first time as $\beta = 15.8 \times 10^{-5}\,^{\circ}C^{-1}$.

1. Introduction

Chitin, poly-β(1 → 4)-*N*-acetyl glucosamine, is synthesized by various organisms, such as insects, crustaceans, mollusks, fungi, yeasts, and algae (Rinaudo, 2006). Second only to cellulose, chitin is the next most abundant natural polymer on earth. Similar to cellulose, it exists in nature as crystalline fibrils that are a few nanometers across. There are two crystalline forms of natural chitin: the major form is α-chitin, and the rarer form is β-chitin (Blackwell, 1973; Rudall, 1963). The crystal structure of these polymorphs has been investigated using X-ray diffraction, FT-IR spectroscopy, and solid-state ^{13}C NMR spectroscopy (Blackwell, 1973; Focher, Naggi, Torri, Cosani, & Terbojevich, 1992; Rudall, 1963; Tanner, Chanzy, Vincendon, Roux, & Gaill, 1990). X-ray diffraction studies have established that these two polymorphs have different packing and arrangement of their molecular chains. α-Chitin adopts a two-chain orthorhombic unit cell with $P2_12_12_1$ symmetry, indicating an antiparallel chain arrangement (Minke & Blackwell, 1978; Sikorski, Hori, & Wada, 2009). On the other hand, β-chitin has a one-chain monoclinic unit cell, with $P2_1$ symmetry, and consists of a parallel chain arrangement (Blackwell, 1969; Gardner & Blackwell, 1975).

It has been known that highly crystalline α-chitin can be obtained from the spines of the phytoplankton, *Phaeocystis* (Chrétiennot-Dinet et al., 1997; Ogawa, Kimura, Wada, & Kuga, 2010) and the grasping spines of arrow worms (Atkins, Dlugosz, & Foord, 1979; Saito, Okano, Chanzy, & Sugiyama, 1995). Recently however, Sikorski et al. (2009) have reported on the relatively resolved and highly orientated X-ray fiber patterns from the tendons of a snow crab (*Chionoecetes opilio*), and thus, have reinvestigated the crystal structure of α-chitin. The model they proposed includes two polymer chains with a 2_1 helix conformation, and an antiparallel arrangement in the orthorhombic unit cell ($a = 0.475$ nm, $b = 1.889$ nm, and $c = 1.033$ nm) with a $P2_12_12_1$ symmetry, the same as the classical model of Minke and Blackwell (1978). However, two distinctive conformations of the C6–O6 hydroxymethyl group, different from that suggested by Minke and Blackwell (1978), and the hydrogen bonding system of α-chitin were demonstrated (Fig. 1).

The utilization of chitin is limited, despite its abundance in nature. To promote the use of chitin, it is important to investigate the structure/property relationships. However, little attention has been paid to this relationship for chitin. One of the important physical properties of the crystalline polymer is the elastic modulus of the crystalline region in the direction parallel to the chain axis (E_l). The E_l value reflects the molecular conformation and the intramolecular hydrogen bonding system in the crystalline

* Corresponding author at: Department of Biomaterials Science, Graduate School of Agricultural and Life Sciences, The University of Tokyo, Tokyo 113-8657, Japan. Tel.: +81 3 5841 5247; fax: +81 3 5841 2677.
E-mail address: awadam@mail.ecc.u-tokyo.ac.jp (M. Wada).

0144-8617/$ – see front matter © 2010 Elsevier Ltd. All rights reserved.
doi:10.1016/j.carbpol.2010.09.025

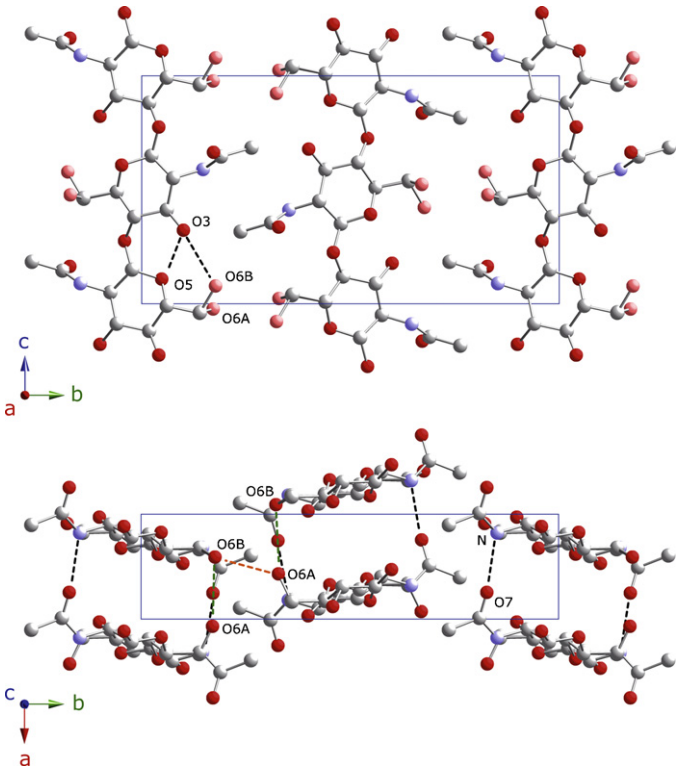

Fig. 1. Crystal structure and unit cell of α-chitin viewed orthogonal to the *bc*-plane (top) and the *ab*-plane (bottom). The dotted lines denote hydrogen bonds (Sikorski et al., 2009).

lattice, and provides the maximum value for a sample modulus of the polymer. However, to the best of our knowledge, only a single paper has reported on the E_l value of α-chitin (Nishino, Matsui, & Nakamae, 1999). The thermal expansion behavior is another important property that is related directly to the molecular arrangement and hydrogen bonding system in the crystalline lattice. However, the thermal expansion behavior reported for α-chitin was only in the lateral directions (Wada & Saito, 2001).

In using synchrotron radiation as an X-ray source instead of conventional Cu Kα radiation, the resolution of the data is enhanced with a much shorter exposure time, because a synchrotron can produce high intensity, directed, and highly monochromatized radiation. Therefore, in this study, the elastic modulus, E_l, and the thermal expansion behavior of α-chitin crystals obtained from the tendons of a snow crab were investigated using synchrotron X-ray diffraction. The results obtained were compared with those obtained from another natural abundant polymer, cellulose.

2. Experimental

2.1. Materials

The snow crab *C. opilio* was boiled in water for a period of 15 min, and the tendons were removed from its body. The tendons were purified by repetitive treatment with 5% KOH and 0.3% $NaClO_2$ solutions, as described previously (Sikorski et al., 2009). The samples were further boiled in a 0.1 N HCl solution for a period of 15 min, and washed in a large volume of deionized water. The purified tendons were finally dried in air while keeping the fiber length constant.

2.2. X-ray diffraction under tensile load

Both ends of the tendon fiber were fixed, with a span of 10 mm, to a pair of cardboard pieces using an epoxy adhesive. Eleven test

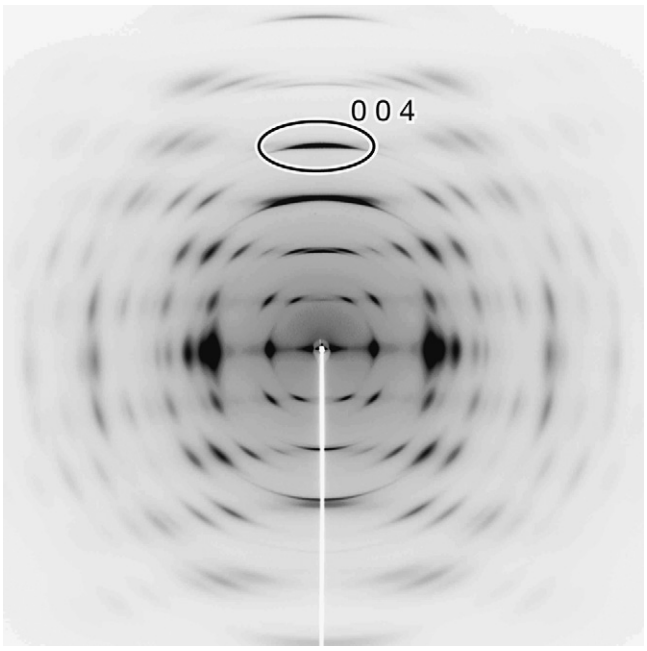

Fig. 2. Synchrotron X-ray fiber diffraction diagram obtained from the tendon of *C. opilio*. The longitudinal axis of the tendon was tilted to satisfy the Bragg condition for the meridional 0 0 4 diffraction.

samples were prepared and installed in the BL40B2 beam line at the SPring-8 synchrotron facility in Japan. The sample was clamped on a goniometer equipped with a stretching device and a load cell (LVS-2KA, Kyowa, Japan), and tilted from the fiber axis at an angle of 11.1° around an axis perpendicular to the fiber direction to comply with the Bragg condition for the meridional 0 0 4 diffraction. Synchrotron-radiated X-rays with a wavelength of 1.0 Å were irradiated on the sample for a period of 30 s at room temperature. A constant tensile load was applied to the sample during the measurements, and increased from 100 gf to 1900 gf in intervals of 100 gf (1 kgf = 9.8 N). The fiber diffraction patterns under set loads were recorded on imaging plates (IPs) (R-Axis IV, Rigaku, Japan). The sample-to-IP distance was calibrated using Si powder (d = 0.31355 nm).

2.3. Degree of orientation

The degree of orientation of the microfibrils was evaluated using Hermans' order parameter (Alexander, 1979):

$$f = \frac{3\langle \cos^2 \phi \rangle - 1}{2} \quad (1)$$

where $\langle \cos^2 \phi \rangle$ denotes the mean-square cosine of the angle between a given crystalline axis and the fiber axis. The parameter f was calculated from the azimuthal profile of the 0 0 4 reflection in the X-ray diffraction diagram of the tendon fiber with the tilted angle of 11.1° around an axis perpendicular to the fiber direction shown in Fig. 2, assuming a cylindrical symmetry.

2.4. Elastic modulus of the crystalline region

The lattice displacements were determined from the d-spacings of the 0 0 4 reflections (d_{004}) from the recorded diffraction patterns. The meridional diffraction profiles were obtained using the Rigaku R-Axis software package. The peak-fitting routine of the X-ray diffraction profiles was carried out using a nonlinear least-squares fitting method (Wada, Okano, & Sugiyama, 1997). A pseudo-Voigt and linear functions were used to fit the 0 0 4 crystallite peaks and

the background profiles, respectively. The d_{004} value under a given load was calculated from the different peak positions. From the changes in the d_{004} value determined, the strain (ε) was calculated using the following formula:

$$\varepsilon = \frac{\Delta d}{d_0} \tag{2}$$

where d_0 is the d_{004} value at a load of 0 N for each sample, and Δd is the difference between the values of d_0 and d_{004} under a given load.

The stress (σ) in the crystalline region was assumed to be equal to the stress applied to the sample, as has been shown experimentally in previous work (Nishino et al., 1999; Nishino, Takano, & Nakamae, 1995). The cross-sectional area of the tendon fiber (A) was measured as follows to evaluate the stress applied to the sample. The fiber was placed between polyethylene sheets and cut along its cross-sectional length. After coating the surface of the sample cross-section with OsO_4, images were recorded using an SEM (Hitachi S4000) and the area, A, was measured using an image analysis software package. The stress was then determined from the load divided by the value of A for each sample. Finally, the elastic modulus of the crystalline region (E_l) was calculated as:

$$E_l = \frac{\sigma}{\varepsilon} \tag{3}$$

where σ is the stress applied to the sample, and ε is the strain.

2.5. X-ray diffraction at elevated temperatures

X-ray fiber diffraction at elevated temperatures was carried out at the BL40B2 beam line at the SPring-8 facility in Japan. The tendon fibers were mounted on a goniometer head with the incident X-ray beam orthogonal to the fiber axis. Synchrotron-radiated X-rays with a wavelength of 0.75 Å irradiated the sample under flowing nitrogen gas for a period of 60 s at a temperature between 50 and 250 °C in steps of 50 °C. The fiber patterns were recorded at the selected temperature using a camera system equipped with a flat imaging plate (IP) (R-Axis IV, Rigaku, Japan). The sample-to-IP distance was calibrated using Si powder (d = 0.31355 nm).

From the recorded fiber patterns, the d-spacings of 28 diffractions were measured using the Rigaku R-Axis software package (Rigaku, Japan). These were indexed according to the orthogonal unit cell of Sikorski et al. (2009), and the unit-cell parameters were determined from the d-spacings and their indices using a least-squares fitting method. The linear and volume thermal expansion coefficients (TECs), α and β, were determined using the following formulae:

$$\alpha = \frac{1}{l_{t=0}} \cdot \frac{\Delta l}{\Delta t} \tag{4}$$

$$\beta = \frac{1}{V_{t=0}} \cdot \frac{\Delta V}{\Delta t} \tag{5}$$

where l is either the d-spacing or the unit cell parameters, V is the volume of the unit cell, and t is the temperature (in °C).

3. Results and discussion

3.1. Elastic modulus

Fig. 2 shows the X-ray fiber diffraction diagram of a tendon of *C. opilio* at a tilt angle of 11.1° around the axis perpendicular to the fiber axis. The diagram in shown in Fig. 2 is a typical pattern of α-chitin, and indicates the high crystallinity and high orientation of the microfibrils. The Hermans' ordered parameter, f, of the tendon was 0.89, evaluated from the meridional 0 0 4 reflection, which is almost the same value as ramie fiber in a naturally highly orientated

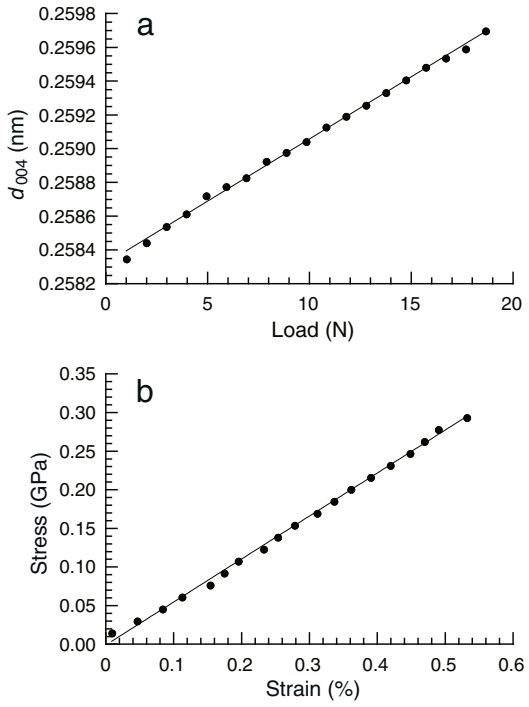

Fig. 3. (a) Changes in the d-spacings of the (0 0 4) plane, d_{004}, when applying a load to a typical tendon sample along its fiber axis. (b) The stress–strain curve obtained from the relationship between the d_{004} value and the load shown in part (a).

cellulose sample (Nishiyama, Kuga, Wada, & Okano, 1997). The high orientation of the microfibrils in our samples supported the internal stress homogeneity in the X-ray experiments under tensile load.

The change in d-spacing (d_{004}) as a function of tensile load for a typical tendon sample is shown in Fig. 3a. The value of d_{004} increased with increasing load applied to the sample, and the relationship between d_{004} and the load was expressed as a straight line. This indicates that the experiment was conducted in the elastic deformation region. From the value of d_{004} and the load relationship (Fig. 3a), the stress–strain curve of the α-chitin crystals shown in Fig. 3b was obtained. The stress of the α-chitin crystals as a function of the tensile strain also showed a linear relationship over the experimental region, and the gradient of the line gave the elastic modulus, E_l, of the α-chitin crystals. The average E_l value of the all the samples tested was 59.3 ± 11.3 GPa, which is about 50% larger than that previously reported of 41 GPa (Nishino et al., 1999). This discrepancy is probably because the stress relaxation that interferes with the precise measurement of the lattice extension under load was restrained in using synchrotron X-ray radiation in this study. Moreover, the degree of crystallinity of the sample in this study was higher than that of the chitin fiber from a crab shell used in a previous paper (Nishino et al., 1999).

The E_l value of the α-chitin in this study, 59.3 ± 11.3 GPa, was less than half of the reported values of another naturally abundant polymer, cellulose, of 137–138 GPa (Nishino et al., 1995; Sakurada, Nukushina, & Ito, 1962). The cross-sectional area of a single molecule in the crystalline lattice (S) of α-chitin (44.9 Å^2) is larger than that of cellulose Iβ (31.7 Å^2) (Nishiyama, Langan, & Chanzy, 2002; Sikorski et al., 2009). The large value of S of α-chitin contributed to the small value of E_l, but the force needed to extend a single molecule of α-chitin and cellulose Iβ had a ratio of 1:1.6. This difference could be considered to be from the molecular conformation and intramolecular hydrogen bonding system of α-chitin and cellulose Iβ (Nishiyama et al., 2002; Sikorski et al., 2009). The fiber repeat of α-chitin (10.33 Å) is smaller than that of cellulose Iβ (10.38 Å), and therefore, the bond angle of the glucosidic linkage is

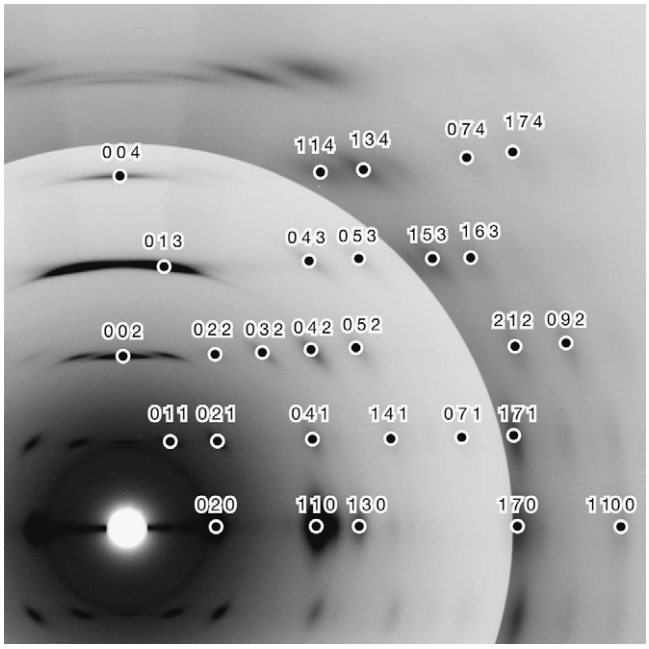

Fig. 4. Synchrotron X-ray fiber diffraction diagram of the tendon of *C. opilio* recorded at 50 °C. Twenty-nine reflections, together with indices used for the calculation of the unit cell parameters, are also shown. The image contrast of the outer region is enhanced to show the weaker reflections more clearly.

smaller: 113.96° for α-chitin and 115.05° for cellulose Iβ. Since the molecular chains of α-chitin are more bent, the crystalline lattice easily expands along the fiber axis direction. There is only one bifurcated intramolecular hydrogen bond, O3–H···O5/O6B, in α-chitin. On the other hand, in cellulose Iβ, two hydrogen bonds, O3–H···O5 and O2–H···O6 or O6–H···O2, resist any extension along the fiber axis direction.

3.2. Thermal expansion

Synchrotron X-ray fiber diffraction diagrams of α-chitin at given temperatures from 50 to 250 °C were recorded. The fiber pattern at 50 °C with markings for 28 diffractions and their indices used for analyses of the thermal expansion behavior is shown in Fig. 4. The unit cell parameters were calculated using a least-squares refinement of the *d*-spacings of these reflections without restraining the included angle of the *a*- and *b*-axes, γ, on taking into account the change in the angle with heating. However, the value of γ was almost constant at 90°: the change in the angle γ between 50 and 250 °C was within 0.2°. This result indicates that the unit cell is consistently orthorhombic in this temperature region. Therefore, the unit cell parameters, *a*, *b*, and *c* at given temperatures, were determined based on the orthorhombic unit cell. These parameters and the volume of the unit cell (*V*) as a function of the temperature are shown in Fig. 5.

The *a*-, *b*-, and *c*-axes increased gradually and linearly with increasing temperature. The linear TECs calculated using Eq. (4) were $\alpha_a = 6.1 \times 10^{-5}\,^{\circ}C^{-1}$, $\alpha_b = 7.3 \times 10^{-5}\,^{\circ}C^{-1}$, and $\alpha_c = 2.1 \times 10^{-5}\,^{\circ}C^{-1}$, respectively. This anisotropic thermal expansion behavior among the *a*-, *b*-, and *c*-axes, $\alpha_b > \alpha_a > \alpha_c$, is ascribed to the crystal structure and to the hydrogen bonding system of α-chitin. α-Chitin greatly expands along the *b*-axis direction, because there is only a single intermolecular hydrogen bond, O6A–H···O6B, which exists along the direction nearly parallel to this direction: i.e., the [1 1 0] direction. Meanwhile, the unit cell expands less along the *a*-axis direction, because two intermolecular hydrogen bonds, N–H···O7 and O6B–H···O6A, exist along this direction. The

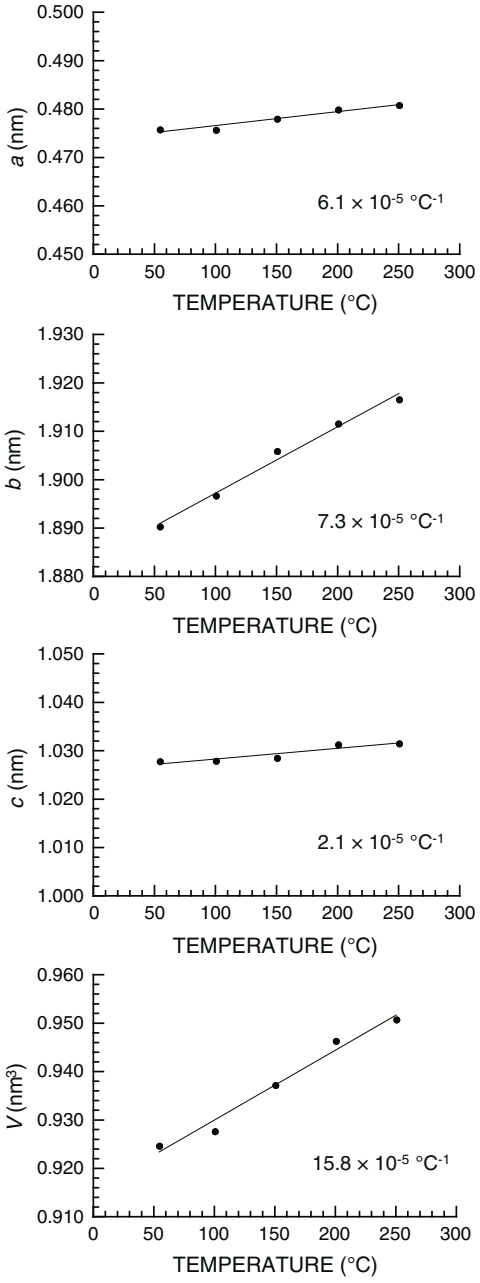

Fig. 5. Changes in the unit cell parameters and volume of α-chitin during heating from 50 to 250 °C under flowing nitrogen. The linear and volume TECs of the α-chitin unit cells are also shown.

values of the TECs were the maximum at the *b*-axes direction and the minimum at the *a*-axes direction in lateral plane of α-chitin crystal. The anisotropy of the TECs of α-chitin is most notable between these two directions. However, this anisotropy in the lateral directions was not remarkable compared with cellulose: $\alpha_b/\alpha_a = 1.2$ and $\alpha_a/\alpha_b = 8.2$ for α-chitin and cellulose Iβ, respectively (Wada, 2002). In cellulose Iβ, all the intermolecular hydrogen bonds exist along the *b*-axis direction, but there are no hydrogen bonds along the *a*-axis direction. α-Chitin hardly expands along the *c*-axis direction, because the extended molecular chains run parallel to this direction, and a bifurcated intramolecular hydrogen bond, O3–H···O5/O6B, further stabilizes the molecule. However, the TEC value was 3.5 times larger than that of cellulose Iβ (Wada, 2002). This is probably because of the fact that two intramolecular hydrogen bonds exist along the *c*-axis direction in cellulose Iβ. In

addition, the fiber repeat of α-chitin is slightly smaller than that of cellulose Iβ (Nishiyama et al., 2002), and therefore, the molecular chains of α-chitin may have room for extending on heating.

The unit-cell volume (V) also showed a linear expansion with increasing temperature (Fig. 5). The volume TEC was calculated using Eq. (5) to be $\beta = 15.8 \times 10^{-5}\,^{\circ}C^{-1}$. This is approximately 1.4 times larger than the reported value of cellulose Iβ of $11.1 \times 10^{-5}\,^{\circ}C^{-1}$ (Hori & Wada, 2005). The volume occupied by a single molecule in the crystalline lattice is smaller, thus α-chitin can expand more easily than can cellulose Iβ.

Acknowledgments

The synchrotron radiation experiments were performed at BL40B2 in SPring-8 with the approval of the Japan Synchrotron Research Institute (JASRI). This study was supported by a Grant-in-Aid for Scientific Research to M.W. (18780131) from the Japanese Ministry of Education, Culture, Sports and Technology, and a research fellowship to R.H. from the Japanese Society for the Promotion of Science.

References

Alexander, L. E. (1979). X-ray diffraction methods. In E. Robert (Ed.), *Polymer science* (pp. 441–452). Humington, New York: Kreiger Publishing Co.

Atkins, E. D. T., Dlugosz, J., & Foord, S. (1979). Electron diffraction and electron microscopy of crystalline α-chitin from the grasping spines of the marine worm Sagitta. *International Journal of Biological Macromolecules*, *1*, 29–32.

Blackwell, J. (1969). Structure of β-chitin or parallel chain systems of poly-β-(1 → 4)-N-acetyl-D-glucosamine. *Biopolymers*, *7*, 281–298.

Blackwell, J. (1973). The polysaccharides. In A. G. Walton, & J. Blackwell (Eds.), *Biopolymers* (pp. 464–513). New York/London: Academic Press.

Chrétiennot-Dinet, M.-J., Giraud-Guille, M.-M., Vaulot, D., Puteaux, J.-L., Saito, Y., & Chanzy, H. (1997). The chitinous nature of filaments ejected by *Phaeocystis* (Prymnesiophyceae). *Journal of Phycology*, *33*, 666–672.

Focher, B., Naggi, A., Torri, G., Cosani, A., & Terbojevich, M. (1992). Structural differences between chitin polymorphs and their precipitates from solution—Evidence from CP-MAS ^{13}C-NMR, FT-IR and FT-Raman spectroscopy. *Carbohydrate Polymers*, *17*, 97–102.

Gardner, K. H., & Blackwell, J. (1975). Refinement of the structure of β-chitin. *Biopolymers*, *14*, 1581–1595.

Hori, R., & Wada, M. (2005). The thermal expansion of wood cellulose crystals. *Cellulose*, *12*, 479–484.

Minke, R., & Blackwell, J. (1978). The structure of α-chitin. *Journal of Molecular Biology*, *120*, 167–181.

Nishino, T., Matsui, R., & Nakamae, K. (1999). Elastic modulus of the crystalline regions of chitin and chitosan. *Journal of Polymer Science Part B: Polymer Physics*, *37*, 1191–1196.

Nishino, T., Takano, K., & Nakamae, K. (1995). Elastic modulus of the crystalline regions of cellulose polymorphs. *Journal of Polymer Science Part B: Polymer Physics*, *33*, 1647–1651.

Nishiyama, Y., Kuga, S., Wada, M., & Okano, T. (1997). Cellulose microcrystal film of high uniaxial orientation. *Macromolecules*, *30*, 6395–6397.

Nishiyama, Y., Langan, P., & Chanzy, H. (2002). Crystal structure and hydrogen-bonding system in cellulose Iβ from synchrotron X-ray and neutron fiber diffraction. *Journal of American Chemical Society*, *124*, 9074–9082.

Ogawa, Y., Kimura, S., Wada, M., & Kuga, S. (2010). Crystal analysis and high-resolution imaging of microfibrillar α-chitin from *Phaeocystis*. *Journal of Structural Biology*, *171*, 111–116.

Rinaudo, M. (2006). Chitin and chitosan: Properties and applications. *Progress in Polymer Science*, *31*, 603–632.

Rudall, K. M. (1963). The chitin/protein complexes of insect cuticles. *Advanced in Insect Physiology*, *1*, 257–313.

Saito, Y., Okano, T., Chanzy, H., & Sugiyama, J. (1995). Structural study of α chitin from the grasping spines of the arrow worm (*Sagitta* spp.). *Journal of Structural Biology*, *114*, 218–228.

Sakurada, I., Nukushina, Y., & Ito, T. (1962). Experimental determination of the elastic modulus of crystalline regions in oriented polymers. *Journal of Polymer Science*, *57*, 651–660.

Sikorski, P., Hori, R., & Wada, M. (2009). Revisit of α-chitin crystal structure using high resolution X-ray diffraction data. *Biomacromolecules*, *10*, 1100–1105.

Tanner, S. F., Chanzy, H., Vincendon, M., Roux, J. C., & Gaill, F. (1990). High-resolution solid-state Carbon-13 nuclear magnetic resonance study of chitin. *Macromolecules*, *23*, 3576–3583.

Wada, M. (2002). Lateral thermal expansion of cellulose Iβ and III_I polymorphs. *Journal of Polymer Science Part B: Polymer Physics*, *40*, 1095–1102.

Wada, M., Okano, T., & Sugiyama, J. (1997). Synchrotron-radiated X-ray and neutron diffraction study of native cellulose. *Cellulose*, *4*, 221–232.

Wada, M., & Saito, S. (2001). Lateral thermal expansion of chitin crystals. *Journal of Polymer Science Part B: Polymer Physics*, *39*, 168–174.